HHS Public Access

Author manuscript

Dev Neurobiol. Author manuscript; available in PMC 2016 December 01.

Published in final edited form as:

Dev Neurobiol. 2015 December ; 75(12): 1441–1461. doi:10.1002/dneu.22294.

Nerve Growth Factor Promotes Reorganization of the Axonal Microtubule Array at Sites of Axon Collateral Branching

Andrea Ketschek[1], **Steven Jones**[2], **Mirela Spillane**[1], **Farida Korobova**[2], **Tatyana Svitkina**[2], and **Gianluca Gallo**[1,*]

[1]Shriners Hospitals Pediatric Research Center, Temple University, Department of Anatomy and Cell Biology, 3500 North Broad St, Philadelphia, PA 19140

[2]University of Pennsylvania, Department of Biology, 433 University Ave, Philadelphia, PA 19104

Abstract

The localized debundling of the axonal microtubule array and the entry of microtubules into axonal filopodia are two defining features of collateral branching. We report that nerve growth factor (NGF), a branch inducing signal, increases the frequency of microtubule debundling along the axon shaft of chicken embryonic sensory neurons. Sites of debundling correlate strongly with the localized targeting of microtubules into filopodia. Platinum replica electron microscopy suggests physical interactions between debundled microtubules and axonal actin filaments. However, as evidenced by depolymerization of actin filaments and inhibition of myosin II, actomyosin force generation does not promote debundling. In contrast, loss of actin filaments or inhibition of myosin II activity promotes debundling, indicating that axonal actomyosin forces suppress debundling. MAP1B is a microtubule associated protein that represses axon branching. Following treatment with NGF, microtubules penetrating filopodia during the early stages of branching exhibited lower levels of associated MAP1B. NGF increased and decreased the levels of MAP1B phosphorylated at a GSK-3β site (pMAP1B) along the axon shaft and within axonal filopodia, respectively. The levels of MAP1B and pMAP1B were not altered at sites of debundling, relative to the rest of the axon. Unlike the previously determined effects of NGF on the axonal actin cytoskeleton, the effects of NGF on microtubule debundling were not affected by inhibition of protein synthesis. Collectively, these data indicate that NGF promotes localized axonal microtubule debundling, that actomyosin forces antagonize microtubule debundling and that NGF regulates pMAP1B in axonal filopodia during the early stages of collateral branch formation.

Keywords

splaying; debundling; bundling; transport; microtubule associated protein 1B; contractility; myosin II; sprout; sprouting; consolidation; GSK3-β

*Corresponding authora: Phone: 215-926-9362, tue86088@temple.edu.

INTRODUCTION

The development of neuronal circuitry relies on the appropriate extension and guidance of axons. However, the ability of neurons to innervate multiple target fields, and form complex arbors within target fields, is limited by the fact that neurons generate a single axon. This limitation is overcome through the de novo formation of axon collateral branches from the main axon (Gibson and Ma, 2011; Gallo, 2011). Furthermore, axon collateralization underlies aspects of the response of the nervous system to injury (Onifer et al., 2011) and thus represents a potential therapeutic target. In the current study, we sought to further understand the cytoskeletal basis of axon collateral branching.

The collateral branches of various types of neurons are initiated as axonal filopodia *in vivo* and *in vitro* (reviewed in Gallo, 2011, 2013). Axons form multiple filopodia, a subset of which matures into branches while the remainder are retracted or fail to mature. Nerve growth factor (NGF) promotes collateral branching along sensory axons by increasing the emergence of axonal filopodia through the regulation of the rate of formation of filopodial precursors termed axonal actin patches (Ketschek and Gallo, 2010; Spillane et al., 2011, 2012; Gallo, 2011, 2013). The maturation of a filopodium into a branch requires that axonal microtubules enter the filopodium and presumably become stabilized, thereby providing cytoskeletal support for the nascent branch, and also allowing the delivery of axonal transport cargoes into the branch (Gallo, 2011; Kalil and Dent, 2014). NGF increases the microtubule content of axons, the polymerization of microtubule plus tips and their targeting into axonal filopodia (Spillane et al., 2012). Thus, during branch formation, NGF regulates both the actin and microtubule cytoskeleton.

Although the basic sequence of cytoskeletal events during branching has been described (Kalil et al, 2000; Dent and Kalil, 2001; Gallo, 2011; Kalil and Dent, 2014), relatively little is known about the mechanisms that locally regulate the dynamics and reorganization of the axonal microtubule array. As the growth cone advances it generates a new segment of axon shaft through a process termed consolidation (Goldberg and Burmeister, 1986; Dent and Gertler, 2003). Consolidation begins at the neck of the growth cone as the axon extends, and actively suppresses protrusive activity along the axon shaft through RhoA-myosin II activity and the degradation of molecules involved in protrusive activity such as cortactin (Loudon et al., 2006; Mignorance-Le Meur and O'Connor, 2009). During consolidation, the splayed microtubules present in the growth cone are bundled into the array of parallel microtubules that characterizes the axon shaft (Burnette et al., 2008). However, for branching to occur the axonal microtubule array must undergo a reorganization from the consolidated state. Thus, signals that promote axon branching likely act, at least in part, by countering the mechanisms of consolidation.

Sites of collateral branching are demarcated by the localized debundling and splaying of the otherwise parallel array of microtubules along the consolidated axon (Dent et al., 1999; Kalil et al., 2000; Dent and Kalil, 2001; Hu et al., 2012). Axonal microtubule plus tips are dynamic undergoing bouts of polymerization and depolymerization. Microtubules can enter into axonal filopodia through either polymerization or transport, and both mechanisms can contribute to branching in a cell type or context dependent manner (Gallo and Letourneau,

1999; Dent and Kalil, 2001). Furthermore, localized fragmentation of long microtubules into smaller fragments may also contribute to branching by providing a supply of mobile microtubules that enter nascent branches through a transport-based mechanism (Yu et al., 1994, 2008; Dent et al., 1999; Gallo and Letourneau, 1999; Qiang et al., 2010). However, the effects of branch-inducing signals on the reorganization of the consolidated axonal microtubule array are not well understood.

This report presents evidence that the branch inducing signal NGF promotes the localized debundling of axonal microtubules, thereby contributing to the formation of axon collateral branches by embryonic sensory neurons. The data also reveal that axonal actomyosin contractility represses the ability of NGF to promote microtubule debundling, and that less microtubule associated protein 1B (MAP1B), which is inhibitory to branching (Bouquet et al., 2004; Dajas-Bailador et al., 2012; Tymanskyj et al., 2012), decorates microtubules entering axonal filopodia during the early stages of NGF-induced branch formation.

METHODS

Culturing, transfection and experimental treatments

Chicken embryonic day (E) 7 explants were cultured on glass substrata coated overnight with 25 μg/mL laminin (Invitrogen) in defined F12H medium (Invitrogen) with supplements as described in Lelkes et al (2006). E7 explants can be cultured on laminin in the absence of NGF and TrkA positive NGF responsive axons extend from the explants, providing a paradigm for the study of the effects of acute NGF treatment (Ketschek and Gallo, 2010; Spillane et al., 2011, 2012, 2013). For experiments involving NGF treatment, cultures were treated with 40 ng/mL NGF (R&D Systems) using treatment times as described in the Results. Controls were similarly treated using NGF vehicle. Blebbistatin (Toronoto Research Chemicals) and latrunculin-A (Sigma) were dissolved in DMSO.

Immunocytochemistry and staining

Two fixation protocols were utilized in this study. In the first protocol (fix then extract), cultures were first fixed with 0.25% glutaraldehyde for 15 min and then permeabilized with 0.1% triton X-100. In the second protocol, designed to reveal the polymeric cytoskeleton independent of soluble proteins, cultures were simultaneously fixed and extracted using a combination of 0.25% glutaraldehyde and 0.1% triton X-100 in cytoskeleton preservation buffer (PHEM buffer) (see Gallo and Letourneau, 1999) for 15 min. In all cases, following fixation/extraction the samples were washed with phosphate buffered saline (PBS) and then treated with 4 mg/mL sodium borohydride to quench glutaraldehyde autofluorescence. The samples were then washed in PBS and blocked in 10% goat serum in PBS containing 0.1% triton X-100 for 15 min, followed by washing three times with PBS. To visualize the cytoskeleton, tubulin and actin filaments were stained using an anti α-tubulin antibody directly conjugated to fluorescein (Sigma; DM1A-FITC, 1:100) and rhodamine phalloidin (Invitrogen; per supplier's directions) for 45 min. All antibodies were diluted in PBS containing 10% goat serum and 0.1% triton X-100. To detect MAP1B we used an antibody kindly supplied by Dr. I. Fischer (Drexel University College of Medicine) (1:400 45 min; Tint et al., 2005) followed by staining with a rhodamine-conjugated secondary antibody

(1:400, Jackson Laboratories). Antibodies to myosin IIA and IIB were obtained from Covance and used at 1:200 (45 min) followed by secondary antibodies as described above (Jackson Laboratories). The anti-pT1265-MAP1B (SuperBUGS) antibody was obtained from Novus Biologicals and used following the protocol described in Trivedi et al (2005) using 0.25% glutaraldehyde as a fixative. Samples were washed three times with PBS containing 10% goat serum and 0.1% triton X-100 between treatment with primary and secondary antibodies. Samples were then washed with PBS three times and mounted using VectaShield (Vector Laboratories).

Quantitative analysis of immunofluorescence

For quantitative immunofluorescence analysis of microtubule and MAP1B levels, all images in data sets to be compared were acquired during the same imaging session using identical imaging parameters established to maintain the signal within the dynamic range. Images were acquired using a Zeiss 200M microscope equipped with a 100× objective (1.3 numerical aperture) and an ORCA ER camera (Hammamatsu) utilizing 1×1 binning. A computer running Zeiss Axiovision software was used to control the microscope and camera during image acquisition. Analysis was performed using Axiovision software. Quantification of total fluorescence intensity was performed as previously described (Spillane et al., 2012). Briefly, a region of interest (ROI) was drawn around the axon and the total integrated pixel values of the signal with the region determined, followed by subtraction of the background signal within the same ROI shifted from the axon onto the adjacent substratum. For ratiometric analysis, the values for the numerator and denominator were similarly obtained.

The extent of pT1265-MAP1B gradients along distal axons was determined by measuring from the tip of the axon to the point where the levels of pT1265-MAP1B became uniform in images with false color lookup tables applied to them (e.g., Figure 6A). The analysis of staining for pT1265-MAP1B in axonal filopodia was performed on fixed then extracted samples in order to image all pT1265-MAP1B in samples counterstained with phalloidin to reveal filopodia. Filopodia between 4-10 μm in length along the distal 50 μm of axons were sampled. This filopodial length range was chosen as it reflect the majority of the filopodial population and minimizes remnants of retracted filopodia and filopodia just emerging from the axon. In order to normalize the pT1265-MAP1B intensity across images for semi-quantitative analysis all images were subjected to “best fit” intensity value modifications using the Image Attributes function in Axiovision software. This manipulation stretched the minimum and maximal pixel intensity values in the image pixel array to cover the dynamic range of image presentation (i.e., lowest pixel value is assigned black and highest pixel value is assigned pure white; see Figure 6F saturation panels). The presence of pT1265-MAP1B staining was then characterized as (−) if no staining was evident, (+/−) if some staining was evident but did not span more than 50% of the filopodial length and (+) if staining was evident along >50% of the fiopodium. In the cases of +/− the staining was usually present within the first few microns of the base of filopodia.

Platinum Replica Electron Microscopy (PREM)

PREM was performed as previously described in Spillane et al (2011), and further detailed in Korobova and Svitkina (2008) and Svitkina (2009). Briefly, cultures of dissociated

neurons were simultaneously fixed and extracted using 0.25% glutaraldehyde and 0.5% Triton X-100 in PEM buffer containing 4 μM jasplakinolide (Calbiochem) and 10 μM taxol (Sigma) for 5 min and postfixed with 2% glutaraldehyde in 0.1 M sodium cacodylate (pH 7.3). Subsequent sample preparation was performed as previously described (Korobova and Svitkina, 2008), Samples were imaged using a JEM 1011 transmission electron microscope (JEOL USA, Peabody, MA) operated at 100 kV. Images were captured by ORIUS 832 10W CCD camera (Gatan, Warrendale, PA) and presented using inverted contrast.

Statistical analysis

All analysis was performed using Graphpad Instat software. The software automatically checks the normalcy of the data distribution. Any sets containing non-normally distributed data were compared using the Mann-Whitney non-parametric test. Normally distributed data sets were compared using Welch t-tests. Categorical data sets were compared using the Chi-squared test performed on the raw categorical data. However, categorical data is presented as percentages in figures.

RESULTS

NGF promotes axon branching and the localized debundling of axonal microtubules along the axon

An acute 30-45 min treatment with NGF promotes the formation of axon collateral branches from embryonic day (E) 7 chicken sensory axons cultured in the absence of NGF. NGF promotes the formation of axonal filopodia (Gallo and Letourneau, 1998; Ketschek and Gallo, 2010; Spillane et al., 2011, 2012), a subset of which mature into collateral branches containing a microtubule core and protrusive structures at their tip and/or along the nascent shaft (Figure 1A). Consistent with our previous studies, a 30 min treatment with NGF promoted the formation of axon collateral branches (Figure 1B), and this treatment protocol was thus used throughout unless otherwise noted. In the absence of NGF treatment, 75% of axons exhibited no collateral branches along the distal 100 μm, compared to 43% following NGF treatment. NGF treatment also increased the relative proportion of axons with one or more branches compared to no NGF treatment (Figure 1B inset).

In order to image the axonal microtubule cytoskeleton using antibodies to α-tubulin without interference from soluble tubulin, samples were simultaneously fixed and extracted (FeX). FeX is a protocol designed to retain polymeric tubulin in microtubules while removing the majority of soluble tubulin (Gallo and Letourneau, 1999). Debundling of the axonal microtubule array was defined as the presence of one or more microtubules that appeared splayed and displaced laterally from the main axonal microtubule array, which otherwise appeared as a solid mass when imaged using epifluorescence microscopy (Figure 1C-G), into the bases of filopodia or splayed domains of the plasma membrane exhibiting protrusions. The microtubules were often curved and displaced lateral to the main array (Figure 1C-E), although they could also exhibit more complex geometries including apparent looping. The presence of microtubule debundling inversely correlated with the length of the branch, which is representative of the time the branch has spent elongating (Gallo and Letourneau, 1999). Branches greater than 30 μm, like the one shown in Figure

1A, often did not show pronounced debundling at their base, while shorter branches exhibited debundling (Figure 1C-E), indicating that microtubule debundling is correlated with the early stages of branch formation and maturation. Following a 30 min treatment with NGF, when new branches are forming, 95% of collateral branches less than 15 μm in length (n=117) exhibited debundled microtubules at their base. In the absence of NGF, 97% of branches less than 15 μm in length (n=39) similarly correlated with sites of microtubule debundling. The relationship between sites of microtubule debundling and the emergence of collateral branches is thus not affected by NGF treatment, indicating that debundling represents a generalized feature of sites of the axon where branches are initiated.

At sites of debundling, microtubules appeared separated from the main array regardless of whether a branch had formed, but almost invariably correlated with the presence of filopodia and/or lamellipodia (analyzed quantitatively in a subsequent section). In regions of the axon shaft exhibiting filopodia and/or lamellipodia, microtubules appeared separated from one another and low alignment was observed on the side of the axon exhibiting the protrusion (Figure 1F,G). The degree of microtubule curvature and apparent number of curved/debundled microtubules varied between sites of debundling, although retaining the same general characteristics. These observations reveal a close relationship between sites representative of the early stages of collateral formation, characterized by axonal protrusive structures, and microtubule debundling.

Counts of the number of sites of localized microtubule debundling along the distal 100 μm of axons revealed that a 30 min treatment with NGF increases the number of sites of debundling by 80% (1.5±0.2 and 2.7±0.2 debundling sites/100 μm of distal axons for no NGF and NGF treatment, respectively; n=123 and 115, $p<0.0001$). NGF also increased the length of axonal segments exhibiting debundled microtubules from 2.9+0.2 μm (n=88) to 6.0+0.5 μm (n=70) ($p<0.0001$). To gain additional insights into the time course of NGF-induced debundling we analyzed the effects of a 5 min treatment with NGF, which precedes the time point when the formation of branches is first observed (Spillane et al., 2012). At the 5 min time point, NGF treated axons exhibited 2.2±0.2 sites of bundling compared to 1.4±0.3 in controls not treated with NGF (n=98 and 106, $p<0.009$). These data reveal that NGF promotes the localized debundling of axonal microtubules prior to the emergence of collateral branches, which occurs between 15-30 min after NGF treatment (Spillane et al., 2012).

Sites of axonal microtubule debundling correlate with the entry of microtubules into filopodia

The entry of microtubules into axonal filopodia is required for the maturation of filopodia into branches (Gallo, 2011; Kalil and Dent, 2014). In order to gain insights into whether debundling may be related to the entry of axonal microtubules into filopodia we analyzed the relationship between sites of debundling and filopodia. In the absence of NGF, only 5% of axonal filopodia were found at sites correlating with debundling (n=203). Following a 30 min NGF treatment, 31% of filopodia correlated with sites of debundling (n=212; $p<0.0001$ relative to no NGF, Fischer's Exact Test). NGF treatment approximately doubles the number of axonal filopodia (Ketschek and Gallo, 2010; Spillane et al., 2012). Since NGF increased

the degree of colocalization of axonal filopodia and sites of debundling by 520% (31%/5%), the increase is not likely attributable to the stochastic association of sites of filopodia formation and debundling. Furthermore, axonal patches of actin filaments serve as precursor structures for the emergence of axonal filopodia (Ketschek and Gallo, 2010; Spillane et al., 2011, 2012, 2013). Analysis of the number of actin patches present at sites of microtubule debundling 30 min post NGF treatment, relative to axon segments of the same length and immediately adjacent to the site of debundling (Figure 1H), revealed that on average sites of bundling exhibited 3.4±0.3 actin patches in contrast to 1.3±0.1 at adjacent sites of the same length (n=49 axons, 106 sites; $p<0.001$). These observations suggest that following NGF-treatment sites of debundling are preferred sites for the formation of axonal filopodia, or that sites of filopodia formation promote debundling.

To further address the relationship between sites of debundling and the formation of axonal filopodia, we determined the percentage of sites of debundling that also exhibited filopodia. In the absence of NGF treatment, 52% of sites of debundling exhibited filopodia (n=85), while following NGF treatment 93% of the sites of debundling exhibited filopodia (n=264) ($p<0.0001$). The entry of microtubules in filopodia was correlated with sites of debundling regardless of NGF treatment. Considering only filopodia that contained microtubules (see Figure 1G for an example of a filopodium containing a microtubule), 88% (n=75) and 91% (n=172) ($p<0.0001$) of filopodia containing microtubules colocalized with sites of microtubule debundling in the absence of NGF and following a 30 min NGF treatment, respectively ($p=0.5$). These observations indicate that the targeting of microtubules into axonal filopodia strongly correlates with the localized debundling of the microtubule array.

In order to gain insights into the ultrastructural relationship of microtubules and actin filaments at sites of axonal microtubule debundling, we relied on platinum replica electron microscopy (PREM). PREM allows high resolution imaging of both actin filaments and microtubules (Svitkina, 2009). Consistent with observations from samples analyzed by immunofluorescence, microtubules at sites of debundling exhibited a curved and splayed morphology (Figure 2 A-E). Curved microtubules also appeared to be in physical contact with, or enmeshed within, actin filament networks found along the axon (Figure 2 A-C). These features of possible links between the actin filament and microtubule cytoskeleton were observed at 23/27 sites of microtubule debundling along NGF treated axons. Collectively, these data reveal that sites of microtubule debundling correlate with the entry of microtubules into axonal filopodia independent of NGF, and that NGF promotes the formation of sites of microtubule debundling along the axon which in turn are associated with sites of NGF-induced filopodial formation and the entry of microtubule tips into filopodia. Sites of microtubule debundling thus appear to be precursor sites for the subsequent microtubule based maturation of collateral branches.

Sites of microtubule debundling do not correlate with a detectable decrease in microtubule content

In cultured central nervous system axons, sites of collateral branch formation correlate with microtubule debundling and the presence of short microtubules considered to be generated by microtubule severing proteins (Yu et al., 1994; Dent et al., 1999; Yu et al., 2008; Qiang et

al., 2010). In order to determine if sites of microtubule debundling along embryonic sensory neuron axons exhibit a net decrease in microtubule polymer levels we measured the total microtubule content at sites of debundling and immediately adjacent segments of the axons of equal length to the site of debundling in axons subjected to FeX. Microtubule content was determined from measurement of the integrated and background subtracted staining intensity of α-tubulin, thus reporting on total microtubule levels (as in Spillane et al., 2012), along axons treated with NGF. This analysis did not reveal detectable net decreases in microtubule polymer levels at sites of debundling ($p>0.8$, $n=72$ debundling sites). We did not qualitatively observe fragmented microtubules (i.e., small individual microtubules) or microtubule tips in the midst of sites of debundling, as also evident in the multiple examples shown throughout this report. These data do not rule out the severing of a few microtubules below the limit of detection of the measurement method, but argue against a wholesale decrease in net microtubule mass at sites of debundling along embryonic sensory axons.

The actomyosin cytoskeleton represses collateral branching and microtubule debundling along the axon

The observation that axonal microtubules at sites of debundling appear in close physical contact with actin filaments (Figure 2) suggested the hypothesis that actin filaments may pull laterally on axonal microtubules, thereby promoting their splaying from the axonal array and debundling. Myosin II is the major actin filament associated motor protein that generates cellular contractile forces. Myosin IIA and IIB heavy chains are present throughout the axon shaft and exhibit a punctate distribution (Figure 3A,B), regardless of NGF treatment. The distributions of myosin IIA and IIB were partially overlapping, as previously described in growth cones (Rochlin et al., 1995). Both myosin IIA and IIB were found in established collateral branches, regardless of NGF treatment (Figure 3B). Myosin IIA exhibited accumulation at the base of axonal filopodia in the absence of and following treatment with NGF (Figure 3C). Myosin IIB often did not exhibit a similar accumulation. Myosin IIA and IIB puncta were also found in the shafts of filopodia along the axon (Figure 3C) and at the growth cone (not shown).

Depolymerization of actin filaments using latrunculin A blocked the formation of axonal filopodia and thus branches (not shown), consistent with previous reports (Gallo and Letourneau, 1998; Dent and Kalil, 2001). Inhibition of myosin II motor activity using blebbistatin, an inhibitor of myosin II ATPase activity (50 μM), increased the formation of collateral branches in response to NGF (30 min cotreatment with NGF; Figure 3D). Blebbistatin treatment did not increase the percentage of axons that formed one or more branches (Figure 3D), but increased the number of collaterals formed per distal 100 μm of axon in axons that formed one or more collaterals (Figure 3D). The effects of blebbistatin treatment on the percentage of axons with 0 to ≥4 collaterals are shown in the inset of Figure 3D. Blebbistatin decreased the percentage of axons that exhibited one collateral by 40% and increased the percentage with 2 to ≥4 branches by 60-80%. Conversely, we over-expressed myosin IIA and IIB heavy chains in dissociated neurons cultured in the presence of NGF and determined the effects on collateral branching. Both myosin IIA and IIB decreased axon branching and the effect of overexpressing myosin II was reversed by culturing in blebbistatin (Figure 3E,F), indicating the overexpressed myosin II suppressed branching

through the activity of its motor domain. Collectively, these results indicate that myosin II activity suppresses NGF-induced axon branching.

Based on the PREM observations revealing that microtubules are enmeshed in actin filaments at the base of filopodia and along the axon (Figure 2), we considered that actin filaments and actomyosin based forces may be involved in pulling microtubules away from the axonal bundle, thus promoting debundling. In contrast to this hypothesis, depolymerization of actin filaments using latrunculin A, or inhibition of myosin II ATPase-dependent motor function using blebbistatin, in conjunction with NGF treatment increased the number of axonal sites of debundling induced by NGF (Figure 4A,B). However, the percentage of filopodia that contained microtubules was not affected by treatment with blebbistatin. As previously reported, treatment with NGF increased the percent of filopodia containing microtubules relative to controls (Spillane et al., 2012; data not shown). In the absence of blebbistatin, 13% (n=256) of axonal filopodia contained one or more microtubules following NGF treatment, compared to 11% (n=118) in the presence of blebbistatin (cotreatment with 50 μM blebbistatin and NGF for 30 min; $p>0.39$). However, blebbistatin treatment increased the distance that microtubules penetrated into filopodia (Figure 4C), as determined by measuring the percentage of the filopodium's length occupied by microtubules. Filopodia were defined using the following criteria to differentiate them from filopodia containing microtubules which had already begun to undergo maturation into a branch; the filopodium must exhibit a linear uniform array of filaments, or exhibit less filament density distally, and have not undergone the early stages of maturation into a branch reflected by lower density of filaments at the base of the filopodium and higher distally (i.e., polarization into a nascent branch). Following NGF treatment, microtubules extended into 44±3.9% (n=47) and 82±2.6%(n=70) ($p<0.0001$) of the length of filopodia in the absence and presence of blebbistatin, respectively. In the presence of blebbistatin, 91% of microtubules penetrated into ≥50% of the filopodium's length, compared to 34% without blebbistatin. Blebbistatin treatment did not affect the length of the filopodia (7.6±0.5 and 6.9±0.4 μm, n=47 and 70 filopodia for control and Blebbistatin treatment, respectively; $p>0.39$). Collectively, these data indicate that actomyosin forces repress the ability of axonal microtubules to become debundled and penetrate along the shafts of axonal filopodia, but do not regulate the entry of microtubules into filopodia. Analysis of the effects of blebbistatin or actin filament depolymerization on the axonal microtubule array and branching in the absence of NGF treatment were not feasible. Unexpectedly, we found that treatment with blebbistatin in the absence of NGF caused rapid cessation of protrusive activity and depolymerization of axonal microtubules (see Supplemental Materials Figure S1).

The effects of NGF on the debundling of axonal microtubules are independent of protein synthesis

The NGF-induced regulation of the actin cytoskeleton underlying the formation of axonal filopodia and axon branching is dependent on NGF-induced intra-axonal protein synthesis (Spillane et al., 2012, 2013). Cycloheximide (CHX) is a translational inhibitor which blocks the effects of NGF on axon branching (Spillane et al., 2012, 2013). A 10 min pretreatment with CHX (35 μM) prior to a 30 min treatment with NGF did not affect the NGF-induced increase in the number of microtubule debundling sites along axons. NGF treated axons

exhibited 2.5±0.2 (n=57) sites of debundling and axons pretreated with CHX and then NGF exhibited 2.7±0.2 (n=60) sites (p=0.19), compared to 1.3±0.3 (n=58) in vehicle treated axons in the absence of NGF treatment. CHX treatment also did not affect the length of axon segments exhibiting sites of NGF-induced debundling (p=0.56, n=70 and 136). As a positive control, CHX prevented the NGF-induced increase in axonal filopodia in the same population of axons (p<0.0002, comparing NGF vs NGF+CHX). These data argue against a role for protein synthesis in the effects of NGF on the debundling of axonal microtubules.

NGF decreases the localization of MAP1B to microtubules during the early phases of collateral formation

Adult dorsal root ganglion neurons from the MAP1B knock out mouse exhibit increased collateral branching (Bouquet et al., 2004). A negative role for MAP1B in branch formation is also supported by studies using embryonic neurons (Tymanskyj et al., 2012; Dajas-Bailador et al., 2012). There is evidence that MAP1B may contribute to the bundling of microtubules albeit likely through indirect mechanisms possibly involving other microtubule associated proteins (Takei et al., 2000; Teng et al., 2001; Noiges et al., 2002; Feltrin et al., 2012), although roles for MAP1B in bundling have not been observed in some studies (Nobles et al., 1989; Takemura et al., 1992; Goold et al., 1999). Furthermore, MAP1B can also regulate aspects of microtubule tip dynamics (Goold et al., 1999; Tymanskyj et al., 2012; Villarroel-Campos D, González –Billault, 2014). However, the mechanistic role of MAP1B in branching is not understood.

In neurons first fixed and then extracted, revealing both soluble and cytoskeleton associated MAP1B, MAP1B was found throughout the axon shaft and within filopodia and branches regardless of NGF treatment, consistent with a previous report (not shown; Bouquet et al., 2004). In order to gain insights into the distribution of MAP1B relative to sites of axonal microtubule debundling, we stained axons that underwent FeX to selectively reveal microtubules and cytoskeleton associated MAP1B. The distribution of cytoskeleton associated MAP1B was determined in control and NGF treated axons. In contrast to fixation followed by extraction, and regardless of NGF treatment, we observed no localization of MAP1B to axonal filopodia unless they contained microtubules in FeX samples, indicating that either the association of MAP1B with actin filaments in filopodia is weak, or that there is no association, and the staining in filopodia not containing microtubules reflects soluble MAP1B (not shown). MAP1B decorated microtubules that underwent splaying and debundling in response to NGF treatment (Figure 5A), and also in the absence of NGF treatment (not shown). Measurements of the ratio of the total integrated and background subtracted staining intensity of MAP1B to α-tubulin in segments of NGF treated axons subjected to FeX that exhibited debundling, relative to the adjacent segments that did not exhibit debundling, did not reveal a decrease in MAP1B levels at the sites of debundling (Figure 5B). Moreover, microtubules with tips that extended laterally from the axonal array were decorated with MAP1B in a microtubule length and NGF-treatment dependent manner (Figure 5C,D). Microtubules that stained positive and negative for MAP1B along their length are denoted as + and − (Figure 5D), respectively, in Figure 5C. Microtubules that exhibited partial coverage by MAP1B (Figure 5D) are denoted as +/−. Following NGF treatment, 28% of microtubules that extended less than 5 μm from the axon shaft exhibited

MAP1B staining. In contrast, in the absence of NGF treatment 91% exhibited MAP1B staining along their length. Following treatment with NGF, the frequency of MAP1B staining increased with increasing microtubule length and the majority of microtubules greater than 15 μm in length exhibited MAP1B staining along their length (Figure 5D). In the absence of NGF treatment, 94-100% of microtubules 5-15 μm in length exhibited MAP1B staining. Following NGF treatment, some microtubules longer than 5 μm exhibited partial MAP1B coverage characterized by a proximo-distal distribution of MAP1B, denoted as +/−. Regardless of NGF treatment, microtubules greater than 15 μm in length, exhibited mostly uniform MAP1B staining (Figure 5C). These observations indicate that sites of microtubule debundling do not correlate with localized decreases in MAP1B levels, but the microtubules that extend outward from the axon shaft into filopodia and collaterals following NGF treatment initially exhibit low levels of MAP1B which however increase with increasing length of the microtubules until they reach levels similar to the axon shaft in fully established mature collaterals. In contrast, in the absence of NGF treatment MAP1B is found along the length of almost all microtubules projecting laterally from the axon shaft (Figure 5C).

In order to determine whether the levels of MAP1B associated with microtubules throughout the axon are changed by treatment with NGF, we compared the ratio of MAP1B to total α-tubulin along the distal 100 μm of axons in cultures that underwent FeX. Treatment with NGF decreased the levels of MAP1B staining relative to tubulin staining (Figure 5E). Axons exhibited ratios of 1.03+0.05 (n=39) and 0.89+0.05 (n=39) in no NGF and NGF treatment groups (30 min), respectively ($p<0.05$). Analysis of the levels of the mean intensity of MAP1B staining in axons fixed and then subsequently extracted, to reveal both cytoskeleton bound and soluble MAP1B, did not reveal a difference between no NGF and NGF treatment groups ($p=0.92$; n=30 and 31, respectively).

Effects of NGF on the levels of MAP1B phosphorylated at Threonine 1265 along the axon shaft

GSK3β is inhibitory to sensory axon branching (Zhao et al., 2009), phosphorylates MAP1B at threonine 1265 (Trivedi et al., 2005) and MAP1B preferentially associates with tyrosinated microtubules (Goold et al., 1999; Tymanskyj et al., 2012) and regulates tubulin tyrosination (Utreras et al., 2008). The levels of pT1265-MAP1B in axons are reported to exhibit a distal (high) proximal (low) gradient (Trivedi et al., 2005). Using the anti pT1265-MAP1B antibody originally characterized by Trivedi et al (2005), gradients were evident along the axons of dissociated neurons fixed and then extracted in no NGF and NGF treated conditions (Figure 6A). Measurement of the length of the gradient, from the axon tip to the point where the intensity of pT1265-MAP1B became uniform, revealed that in neurons treated with NGF the gradient was approximately 40% longer ($p<0.0001$, Mann-Whitney test; Figure 6A). However, analysis of the total staining intensity of pT1265-MAP1B in fixed and then extracted samples along the distal 50 μm of the axon shaft, defined by the microtubule array (Figure 6B inset), did not reveal an effect of treatment with NGF on the local levels of pT1265-MAP1B (Figure 6B; $p=0.84$, n=57 and 50 axons for no NGF and NGF groups). Thus, NGF increases the coverage of the axon shaft by pT1265-MAP1B

(Figure 6A) but does not affect the levels of pT1265-MAP1B within a defined segment of the axon shaft.

Analysis of the distribution of pT1265-MAP1B associated with microtubules protruding from the axon shaft (in FeX samples) showed that treatment with NGF decreased the proportion of microtubules that exhibited pT1265-MAP1B staining (Figure 6C,D), consistent with the observations on total MAP1B (Figure 5C,D). In no NGF and NGF alike, the majority of microtubules or bundles of microtubules extending further than 15 μm from the axon shaft exhibited pT1265-MAP1B staining (Figure 6C), again consistent with the observations on total MAP1B. Similarly, established collaterals exhibited pT1265-MAP1B staining (Figure 6E).

As with total MAP1B, pT1265-MAP1B staining was observed along microtubules at sites of debundling (Figure 6C, denoted by } in NGF treated panel). Analysis of the ratio of pT1265-MAP1B/tubulin total intensities in FeX samples at regions of debundling and adjacent axon segments of the same length in NGF treated samples (as previously described in Figure 5B) did not reveal any differences (0.90±0.06 and 0.97±0.07, respectively. n=19. Welch t-test, p=0.44). Thus, NGF does not affect the levels of MAP1B or its phosphorylation at pT1265 along microtubules within axon segments exhibiting debundling.

Effects of NGF treatment on the levels of pT1265-MAP1B at axonal filopodia

Although NGF did not affect the net levels of pT1265-MAP1B along the axon shaft as defined by the microtubule array (Figure 6B), scrutiny of data sets suggested localized differences in the levels of pT1265-MAP1B within axonal filopodia. In samples fixed and then extracted, thus revealing total pT1265-MAP1B, and counter-stained to reveal actin filaments, treatment with NGF resulted in decreased levels of pT1265-MAP1B staining in filopodia relative to no NGF treatment (Figure 6F). Analysis of the percentage of filopodia containing pT1265-MAP1B showed that NGF treatment decreased the percentage of filopodia exhibiting high levels of pT1265-MAP1B and increased the percentage of filopodia not exhibiting pT1265-MAP1B staining (Figure 6G,H).

Levels of acetylated tubulin in microtubules projecting in axonal filopodia and nascent branches

The initial stabilization of microtubules in axonal filopodia is considered to contribute to the subsequent maturation of the filopodium into a branch (Gallo, 2011; Kalil and Dent, 2014). Since MAP1B promotes microtubule tip polymerization (Tymanskyj et al., 2012) decreased levels of MAP1B along axonal microtubules penetrating filopodia may correlate with microtubule stability. Stabilized microtubules exhibit increased levels of detyrosinated and acetylated α-tubulin, post-translational modifications which correlate with stability (Janke, 2014). We previously reported that in the presence of NGF approximately 40% of microtubules less than 10 μm in length projecting into axonal protrusions exhibit detyrosinated tubulin (Gallo and Letourneau, 1999). Analysis of the percentage of microtubules projecting outward from the axon shaft positive for acetylated tubulin in FeX samples similarly indicates that approximately 60% of microtubules less than 10 μm in length also contain acetylated tubulin (Supplemental Materials, Figure S2). Collectively, the

observations indicate a correlation between the levels of MAP1B on microtubules during the early stages of branching and stability of subsets of microtubules entering axonal filopodia.

DISCUSSION

The mechanism of axon consolidation, which suppresses protrusive activity and branching from the axon shaft, is poorly understood. This study unveils aspects of the mechanism that maintains the axonal microtubule array consolidated, and negatively regulates the formation of collateral branches. The data indicate that actomyosin forces along the axon act to suppress microtubule debundling and reorganization, thereby promoting the maintenance of a uniform microtubule array within the consolidated axon. This study also indicates that the association of MAP1B with axonal microtubules penetrating axonal filopodia is likely to contribute to the inhibitory role of MAP1B in axon branching (Bouquet et al., 2004; Tymanskyj et al., 2012). Both of these aspects of axonal microtubules are altered by treatment with NGF. Figure 7A provides a diagram of the temporal sequence of cytoskeletal events currently known to underlie the formation of sensory axon collateral branches in response to NGF. The promotion of the debundling of axonal microtubules precedes other major events such as the increase in the formation of actin patches, emergence of filopodia from patches and the maturation of branches from filopodia.

Inhibition of myosin II increased the number of NGF-induced branches generated per axon. NGF partially inhibits myosin II activity (Fujita et al., 2001), myosin II represses the formation of axonal filopodia along the distal axon (Loudon et al., 2006) and in growth cones myosin II antagonizes the ability of microtubules to penetrate along the shafts of filopodia (Myers et al., 2006; Burnette et al., 2007; Ketschek et al., 2007). The current data reveal a novel role of axonal actomyosin contractility, the regulation of the localized debundling of the microtubule cytoskeleton along the consolidated axon shaft. At the growth cone neck, the site where axon consolidation initially occurs, myosin II forces similarly assist in bundling splayed microtubules in the growth cone during axon advance (Burnette et al., 2008). The data suggest that myosin II, acting on the cortical actin cytoskeleton, generates compressive forces which normally antagonize the ability of microtubules to debundle and splay. Although not yet detailed in sensory axons, super-resolution imaging of the the consolidated axons of developing hippocampal neurons in vitro revealed periodic rings of subcortical actin filaments that envelope the underlying microtubule cytoskeleton (Xu et al., 2013; Gallo, 2013b; D'Este et al., 2015). Myosin II may drive the contractility of these rings around the axonal microtubule array thus serving to promote the bundling of microtubules. Myosin II contractility along the axon also inhibits the advance of microtubules into axonal filopodia, a role conserved at the growth cone. Thus, this study indicates that myosin II antagonizes not only the initial actin filament based step in branch formation, the formation of axonal filopodia, but also the process of branch maturation by attenuating microtubule debundling and the ability of microtubules to penetrate axonal filopodia.

The mechanistic function of the localized debundling of axonal microtubules in axon branching is not clear. This study identifies that sites of debundling strongly correlate (88-91%) with sites where axonal microtubules invade axonal filopodia, independent of

NGF treatment. Thus, the debundling may assist microtubule plus tips in targeting to filopodia. In the absence of debundling, axonal microtubules are organized into a parallel array and a microtubule tip entering an axonal filopodia would need to make a near orthogonal turn into the filopodium. Localized debundling may thus promote the ability of microtubules to target into filopodia by changing the orientation of microtubule tips relative to the base of filopodia (Figure 7B). This would be particularly significant if the microtubule tips in the axon were growing along the shafts of pre-existing microtubules, the curvature of which would then allow for easier engagement of the growing microtubule tip with the base of the filopodium.

We also report that actin filaments along the axon exhibit what appears to be physical contacts with microtubules that are debundled from the main array. Thus, the interplay between actin filaments and debundled microtubules may further promote interactions between growing microtubule tips and the actin filaments in filopodia and their actin patch precursors. Along these lines, the actin filament associated septin 7 (Spiliotis and Nelson, 2006; Hagiwara et al., 2006; Roth et al., 2013) targets to the base of filopodia and promotes the targeting of microtubules into axonal filopodia (Hu et al., 2012) and also localizes to domains of the axon exhibiting debundling (Hu et al., 2012). Similarly, drebrin is a protein that associates with actin filaments and can also bind microtubule tips through end binding proteins (Geraldo et al., 2008). Previous work implicates drebrin as a positive regulator of axon branching (Dun et al., 2012). In unpublished work, we find that drebrin targets predominantly to the base and proximal portion of axonal filopodia (data not shown; see Gallo, 2013 for a preliminary example), indicating it may also promote the entry or retention of microtubules during the early phases of collateral branching. Thus, molecules that mediate actin-microtubule interactions are located at the base of filopodia corresponding to sites of microtubule debundling, and the observed physical interactions between filaments and microtubules may reflect the activity and localization of these proteins. However, we cannot exclude that the observed apparent physical contacts between microtubules and actin filaments may also reflect fixation-induced cross-linking between actin filaments and microtubules.

Following a 30 min NGF treatment sites of microtubule debundling correlated with the presence of filopodia. We have previously reported that a 30-45 min NGF treatment induces a colocalization of sites of formation of axonal filopodia and actin patches with stalled mitochondria (Ketschek and Gallo, 2010; Spillane et al., 2013). Collectively these observations suggest that sites of microtubule debundling may also correlate with the presence of mitochondria. The induction of axonal filopodia and actin patches by NGF is evident after approximately 15 min of treatment (Spillane et al., 2012; Figure 7A). This delayed response to NGF likely reflects the dependence of the NGF-induced axonal filopodia on NGF-induced intra-axonal protein synthesis of actin regulatory proteins at sites of the axon populated by mitochondria (Spillane et al., 2012, 2013). However, NGF induced debundling of microtubules by five minutes following treatment, suggesting that the debundling of microtubules may be an early response of the axon with functions in reorganizing the axonal cytoplasm (e.g., organelle targeting to potential branching sites). Indeed, sites of branch formation correlate with the targeting of vesicles and branching is regulated by motor driven processes (Ponomareva et al., 2014; Sainath and Gallo, 2014).

Mechanistically, a possible function for microtubule debundling may be to promote the stalling or capture of axonal transport cargoes using microtubule based mechanisms. The curvature of the microtubules at sites of debundling may adversely affect the ability of cargoes to undergo movement along microtubules (Figure 7B). To our knowledge, the effects of microtubule curvature on motor protein based transport have not been addressed. However, in the context of the dynein-dependent bending of flagella during their beating cycle, the curvature of the microtubules has been considered as a mechanism that regulates dynein activity (e.g., Brokaw, 2009; Cibert and Ludu, 2010). In this system, it has been proposed that dynein activity on the convex side of the flagellum is decreased. If curvature does affect anterograde or retrograde motor protein based transport then it may contribute to the accumulation of transport cargoes (e.g., mitochondria) at sites of branching (Courchet et al., 2013; Spillane et al., 2013; Ponomareva et al., 2014; Tao et al., 2014).

NGF-induced branching requires the NGF-induced intra-axonal synthesis of regulators of the actin cytoskeleton (Spillane et al., 2012,2013). Consistent with our prior study, which failed to reveal a role for intra-axonal protein synthesis in the NGF-induced increase in axonal microtubule polymer levels or the targeting of microtubules into axonal filopodia (Spillane et al., 2012), we similarly did not detect a role for protein synthesis in the NGF-induced debundling of axonal microtubules. Furthermore, NGF promoted the debundling of axonal microtubules following a five minute treatment, and this fast response is not immediately consistent with a mechanism involving protein synthesis in these axons (Spillane et al., 2012). Similarly, NGF was not found to affect the levels of MAP1B in axons, indicating it does not regulate its axonal translation. While intra-axonal protein synthesis dependent regulation of some yet to be addressed aspect of the axonal microtubule cytoskeleton by NGF cannot be ruled out, the data thus far indicate that NGF does not rely on intra-axonal protein synthesis to regulate fundamental aspects of the microtubule-based components of the branching of sensory axons.

MAP1B is a negative regulator of the branching of adult sensory (Bouquet et al., 2004) and embryonic central nervous system axons (Tymanskyj et al., 2012). Consideration of the distribution and levels of MAP1B along the axon and at sites of microtubule debundling did not reveal decreases in MAP1B or pT1265-MAP1B associated with microtubules. This observation argues against a role for net MAP1B levels or pT1265-MAP1B in contributing to the localized debundling of axonal microtubules. However, analysis of the association of MAP1B/pT1265-MAP1B with microtubules penetrating axonal filopodia indicates that under conditions when branching is promoted (e.g., NGF treatment) the association of MAP1B with microtubules is decreased during the early phases of branching. Subsequently, as the branch matures and attains greater length, the levels of MAP1B and pT1265-MAP1B along microtubules in branches increase. NGF treatment also correlated with a 14% decrease in the ratio of MAP1B to microtubule mass throughout the axon shaft, without affecting total levels of axonal MAP1B. However, NGF induces an increase in the total amount of microtubule polymer in axons (Spillane et al., 2012), and thus the observed slight decrease in the association of MAP1B with microtubules may be reflective of an increase in microtubule levels in the absence of a correlated increase in MAP1B levels or the proportion of MAP1B that is able to bind microtubules within the axon shaft.

NGF increased the length of the gradient of pT1265-MAP1B along the distal axon but did not affect the levels of pT1265-MAP1B locally within the distal axon shaft. The observation that NGF increases the length of the gradient is consistent with prior reports that NGF increases the net levels of pT1265-MAP1B detected through whole cell biochemical analysis (Goold and Gordon-Weeks, 2001, 2003, 2005). The effect of NGF on extending the pT1265-MAP1B gradient is likely due to activation of the MAPK pathway in the axon shaft (Goold and Gordon-Weeks, 2005). In contrast to the main axon shaft, the data indicate that NGF decreases the phosphorylation of MAP1B at the pT1265 GSK-3β phosphorylation site specifically in axonal filopodia. In primary sensory neurons NGF increases the level of inactive GSK-3β, as revealed by biochemical analysis of the levels of S9 phosphorylation (pS9-GSK-3β; Zhao et al., 2009), a site under regulation by Akt and other kinases which upon phosphorylation inactivates GSK-3β (Kaidanovich-Beilin O, Woodgett, 2011). Through imaging of PI3K signaling in living sensory axons, we have previously reported that NGF induces PI3K signaling locally within axonal filopodia (Ketschek and Gallo, 2010). Thus, the localized decrease in the levels of pT1265-MAP1B in axonal filopodia induced by NGF may reflect the localized activation of PI3K-Akt signaling resulting in local inactivation of GSK-3β (Figure 7C). Furthermore, inactivated pS9-GSK-3β if found in the filopodia of E7 chicken sensory neurons raised in NGF in a PI3K dependent manner (Eickholt et al., 2002), the same neuronal population used in the current study. Future consideration of the distribution of GSK-3β and inactivated pS9-GSK-3β along the axon shaft and within axonal filopodia may reveal additional details on the possible subcellular regulation of this kinase, and its substrates (e.g., MAP1B), by NGF. Consistent with the notion of localized signaling in different domains of the axon, PI3K-Akt signaling locally inactivates GSK3-β through S9 phosphorylation in the peripheral domain of embryonic sensory growth cones, and the levels of activated GSK3-β are higher in the axon shaft relative to the growth cone (Zhou et al, 2004).

Collectively, the results suggest that NGF differentially affects the phosphorylation of MAP1B within the main axon shaft and the laterally projecting filopodia. In the context of branching, this may reflect NGF-induced promotion of microtubule plus tip polymerization within the axon shaft (as observed in Spillane et al., 2012), allowing more microtubule tips to search for and penetrate axonal filopodia (Spillane et al., 2012). However, when microtubules become targeted to filopodia, local signaling decreases the phosphorylation of MAP1B associated with microtubule tips during early stages of branching. MAP1B promotes the polymerization of microtubule plus tips (reviewed in Villarroel-Campos and Gonzalez-Billault, 2014). Thus, the observed decreased levels of MAP1B and its phosphorylated form on microtubules during the early stages of branch formation within axonal filopodia may reflect a mechanism which contributes to the stabilization of microtubules in nascent branches (Figure 7D). Once the branch matures and polarizes, the PI3K-Akt inhibitory mechanism could also become polarized to the rip of the branch, as observed along the main axon (Zhou et al, 2004), and MAP1B may then be recruited to microtubules to serve a similar function as in the extension of the main axon shaft (i.e., the promotion of microtubule dynamics as the branch now extends independently of the main axon; Tymanskyj et al., 2012). Consistent with this notion, the filopodia of MAP1B KO adult sensory axons exhibit more frequent stabilization and maturation into branching

(Bouquet et al., 2004). However, some studies report that MAP1B promotes stabilization of microtubules (Tint et al., 2005; Bondallaz et al., 2006), indicating the function of MAP1B may be context dependent and that possibly in the context of branching the absence of MAP1B from microtubules penetrating filopodia may reflect a mechanism aimed to increase their dynamics in filopodia. This possibility is argued against by the relatively high numbers of acetylated and detyrosinated microtubule tips found in axonal filopodia. Future studies in MAP1B depleted/KO neurons directly imaging microtubule dynamics in axonal filopodia will be required to clarify this issue.

Additionally, axonal mitochondria exhibit near doubled velocities of retrograde transport in MAP1B KO neurons (Jimenez-Mateos et al., 2006). Mitochondria target to branches once the branches have attained lengths comparable to those observed to correlate with MAP1B binding to microtubules in the presence of NGF (Spillane et al., 2013). This correlation suggests that the decreased levels of MAP1B on microtubules during the early phases of branch formation may serve to prevent the entry of mitochondria into branches that have not yet sufficiently matured by promoting their retrograde movement. MAP1B can also positively regulate Rac1 activity through regulation of the TIAM1 GEF (Montenegro-Venegas et al., 2010; Henriquez et al., 2012). Rac1 is involved in the formation of branches along sensory axons through the positive regulation of WAVE1-mediated activation of the Arp2/3 actin nucleation complex, which drives the formation of the axonal actin patches from which filopodia emerge (Spillane et al., 2012). Rac1 is also required for integrin-dependent extension of the main axon and generally promotes axon branching (Kuhn et al., 1998; Spillane and Gallo, 2014). If MAP1B is involved in the regulation of Rac1 during axon branching, which remains to be addressed, then it is likely to have a role during the later stages of branch extension in a manner similar to that for extension of the main axon. MAP1B may however also contribute to the Rac1 mediated formation of axonal actin patches along the axon shaft (Spillane et al., 2012).

Supplementary Material

Refer to Web version on PubMed Central for supplementary material.

Acknowledgments

AK and SJ contributed equally to this manuscript. This work was supported by awards to GG (NIH NS078030) and TS (NIH GM095977). We thank Dr. I. Fischer (Drexel University College of Medicine) for providing MAP1B antibodies and constructive suggestions made by the reviewers.

REFERENCED LITERATURE

Ahmad FJ, He Y, Myers KA, Hasaka TP, Francis F, Black MM, Baas PW. Effects of dynactin disruption and dynein depletion on axonal microtubules. Traffic. 2006; 7:524–37. [PubMed: 16643276]

Bondallaz P, Barbier A, Soehrman S, Grenningloh G, Riederer BM. The control of microtubule stability in vitro and in transfected cells by MAP1B and SCG10. Cell Motil Cytoskeleton. 2006; 63:681–95. [PubMed: 17009328]

Bouquet C, Soares S, von Boxberg Y, Ravaille-Veron M, Propst F, Nothias F. Microtubule-associated protein 1B controls directionality of growth cone migration and axonal branching in regeneration of adult dorsal root ganglia neurons. J Neurosci. 2004; 24:7204–13. [PubMed: 15306655]

Brokaw CJ. Thinking about flagellar oscillation. Cell Motil Cytoskeleton. 2009; 66:425–36. [PubMed: 18828155]

Burnette DT, Schaefer AW, Ji L, Danuser G, Forscher P. Filopodial actin bundles are not necessary for microtubule advance into the peripheral domain of Aplysia neuronal growth cones. Nat Cell Biol. 2007; 9:1360–9. [PubMed: 18026092]

Burnette DT, Ji L, Schaefer AW, Medeiros NA, Danuser G, Forscher P. Myosin II activity facilitates microtubule bundling in the neuronal growth cone neck. Dev Cell. 2008; 15:163–9. [PubMed: 18606149]

Cibert C, Ludu A. Is the curvature of the flagellum involved in the apparent cooperativity of the dynein arms along the “9+2” axoneme? J Theor Biol. 2010; 265:95–103. [PubMed: 20399794]

Courchet J, Lewis TL Jr, Lee S, Courchet V, Liou DY, Aizawa S, Polleux F. Terminal axon branching is regulated by the LKB1-NUAK1 kinase pathway via presynaptic mitochondrial capture. Cell. 2013; 153:1510–25. [PubMed: 23791179]

D’Este E, Kamin D, Göttfert F, El-Hady A, Hell SW. STED Nanoscopy Reveals the Ubiquity of Subcortical Cytoskeleton Periodicity in Living Neurons. Cell Rep. 2015; 10:1246–51. [PubMed: 25732815]

Dajas-Bailador F, Bonev B, Garcez P, Stanley P, Guillemot F, Papalopulu N. microRNA-9 regulates axon extension and branching by targeting Map1b in mouse cortical neurons. Nat Neurosci. 2012; 15:697–699.

Dent EW, Callaway JL, Szebenyi G, Baas PW, Kalil K. Reorganization and movement of microtubules in axonal growth cones and developing interstitial branches. J Neurosci. 1999; 19:8894–908. [PubMed: 10516309]

Dent EW, Kalil K. Axon branching requires interactions between dynamic microtubules and actin filaments. J Neurosci. 2001; 21:9757–69. [PubMed: 11739584]

Dent EW, Gertler FB. Cytoskeletal dynamics and transport in growth cone motility and axon guidance. Neuron. 2003; 40:209–27. [PubMed: 14556705]

Dun XP, Bandeira de, Lima T, Allen J, Geraldo S, Gordon-Weeks P, Chilton JK. Drebrin controls neuronal migration through the formation and alignment of the leading process. Mol Cell Neurosci. 2012; 49:341–50. [PubMed: 22306864]

Eickholt BJ, Walsh FS, Doherty P. An inactive pool of GSK-3 at the leading edge of growth cones is implicated in Semaphorin 3A signaling. J Cell Biol. Apr 15; 2002 157(2):211–7. 2002. [PubMed: 11956225]

Feltrin D, Fusco L, Witte H, Moretti F, Martin K, Letzelter M, Fluri E, Scheiffele P, Pertz O. Growth cone MKK7 mRNA targeting regulates MAP1b-dependent microtubule bundling to control neurite elongation. PLoS Biol. 2012; 10:e1001439. [PubMed: 23226105]

Fujita A, Hattori Y, Takeuchi T, Kamata Y, Hata F. NGF induces neurite outgrowth via a decrease in phosphorylation of myosin light chain in PC12 cells. Neuroreport. 2001; 12:3599–602. [PubMed: 11733719]

Gallo G. The cytoskeletal and signaling mechanisms of axon collateral branching. Dev Neurobiol. 2011; 71:201–20. [PubMed: 21308993]

Gallo G. Mechanisms underlying the initiation and dynamics of neuronal filopodia: from neurite formation to synaptogenesis. Int Rev Cell Mol Biol. 2013; 301:95–156. [PubMed: 23317818]

Gallo G. More than one ring to bind them all: recent insights into the structure of the axon. Dev Neurobiol. 2013b; 73:799–805. [PubMed: 23784998]

Gallo G, Letourneau PC. Localized sources of neurotrophins initiate axon collateral sprouting. J Neurosci. 1998; 18:5403–14. [PubMed: 9651222]

Gallo G, Letourneau PC. Different contributions of microtubule dynamics and transport to the growth of axons and collateral sprouts. J Neurosci. 1999; 19:3860–73. [PubMed: 10234018]

Geraldo S, Khanzada UK, Parsons M, Chilton JK, Gordon-Weeks PR. Targeting of the F-actin-binding protein drebrin by the microtubule plus-tip protein EB3 is required for neuritogenesis. Nat Cell Biol. 2008; 10:1181–9. [PubMed: 18806788]

Gibson DA, Ma L. Developmental regulation of axon branching in the vertebrate nervous system. Development. 2011; 138:183–95. [PubMed: 21177340]

Goldberg DJ, Burmeister DW. Stages in axon formation: observations of growth of Aplysia axons in culture using video-enhanced contrast-differential interference contrast microscopy. J Cell Biol. 1986; 103:1921–31. [PubMed: 3782290]

Goold RG, Owen R, Gordon-Weeks PR. Glycogen synthase kinase 3beta phosphorylation of microtubule-associated protein 1B regulates the stability of microtubules in growth cones. J Cell Sci. 1999; 112:3373–84. [PubMed: 10504342]

Goold RG, Gordon-Weeks PR. Microtubule-associated protein 1B phosphorylation by glycogen synthase kinase 3beta is induced during PC12 cell differentiation. J Cell Sci. 2001; 114:4273–84. [PubMed: 11739659]

Goold RG, Gordon-Weeks PR. NGF activates the phosphorylation of MAP1B by GSK3beta through the TrkA receptor and not the p75(NTR) receptor. J Neurochem. 2003; 87:935–46. [PubMed: 14622124]

Goold RG, Gordon-Weeks PR. The MAP kinase pathway is upstream of the activation of GSK3beta that enables it to phosphorylate MAP1B and contributes to the stimulation of axon growth. Mol Cell Neurosci. 2005; 28:524–34. [PubMed: 15737742]

Gordon-Weeks PR. Organization of microtubules in axonal growth cones: a role for microtubule-associated protein MAP 1B. J Neurocytol. 1993; 22:717–25. [PubMed: 8270956]

Hagiwara A, Tanaka Y, Hikawa R, Morone N, Kusumi A, Kimura H, Kinoshita M. Submembranous septins as relatively stable components of actin-based membrane skeleton. Cytoskeleton. 2011; 68:512–25. [PubMed: 21800439]

Henríquez DR, Bodaleo FJ, Montenegro-Venegas C, González-Billault C. The light chain 1 subunit of the microtubule-associated protein 1B (MAP1B) is responsible for Tiam1 binding and Rac1 activation in neuronal cells. PLoS One. 2012; 7:e53123. [PubMed: 23300879]

Hu J, Bai X, Bowen JR, Dolat L, Korobova F, Yu W, Baas PW, Svitkina T, Gallo G, Spiliotis ET. Septin-driven coordination of actin and microtubule remodeling regulates the collateral branching of axons. Curr Biol. 2012; 22:1109–15. [PubMed: 22608511]

Jiménez-Mateos EM, González-Billault C, Dawson HN, Vitek MP, Avila J. Role of MAP1B in axonal retrograde transport of mitochondria. Biochem J. 2006; 397:53–9. [PubMed: 16536727]

Kaidanovich-Beilin O, Woodgett JR. GSK-3: Functional Insights from Cell Biology and Animal Models. Front Mol Neurosci. 2011; 16(4):40. [PubMed: 22110425]

Kalil K, Szebenyi G, Dent EW. Common mechanisms underlying growth cone guidance and axon branching. J Neurobiol. 2000; 44:145–58. [PubMed: 10934318]

Kalil K, Dent EW. Branch management: mechanisms of axon branching in the developing vertebrate CNS. Nat Rev Neurosci. 2014; 15:7–18. [PubMed: 24356070]

Ketschek AR, Jones SL, Gallo G. Axon extension in the fast and slow lanes: substratum-dependent engagement of myosin II functions. Dev Neurobiol. 2007; 67:1305–20. [PubMed: 17638383]

Ketschek A, Gallo G. Nerve growth factor induces axonal filopodia through localized microdomains of phosphoinositide 3-kinase activity that drive the formation of cytoskeletal precursors to filopodia. J Neurosci. 2010; 30:12185–97. [PubMed: 20826681]

Korobova F, Svitkina T. Arp2/3 complex is important for filopodia formation, growth cone motility, and neuritogenesis in neuronal cells. Mol Biol Cell. 2008; 19:1561–74. [PubMed: 18256280]

Kuhn TB, Brown MD, Bamburg JR. Rac1-dependent actin filament organization in growth cones is necessary for beta1-integrin-mediated advance but not for growth on poly-D-lysine. J Neurobiol. 1998; 37:524–40. [PubMed: 9858256]

Lelkes, PI.; Unsworth, BR.; Saporta, S.; Cameron, DF.; Gallo, G. Culture of Neuroendocrine and Neuronal Cells for Tissue Engineering. In: Vunjak-Novakovic, G.; Freshney, RI., editors. Culture of Cells for Tissue engineering. Wiley Inc.; New York: 2006. Chapter 14

Loudon RP, Silver LD, Yee HF Jr, Gallo G. RhoA-kinase and myosin II are required for the maintenance of growth cone polarity and guidance by nerve growth factor. J Neurobiol. 2006; 66:847–67. [PubMed: 16673385]

Mingorance-Le Meur A, O'Connor TP. Neurite consolidation is an active process requiring constant repression of protrusive activity. EMBO J. 2009; 28:248–60. [PubMed: 19096364]

Montenegro-Venegas C, Tortosa E, Rosso S, Peretti D, Bollati F, Bisbal M, Jausoro I, Avila J, Cáceres A, Gonzalez-Billault C. MAP1B regulates axonal development by modulating Rho-GTPase Rac1 activity. Mol Biol Cell. 2010; 21:3518–28. [PubMed: 20719958]

Myers KA, Tint I, Nadar CV, He Y, Black MM, Baas PW. Antagonistic forces generated by cytoplasmic dynein and myosin-II during growth cone turning and axonal retraction. Traffic. 2006; 7:1333–51. [PubMed: 16911591]

Preitner, Nicolas; Quan, Jie; Nowakowski, Dan W.; Hancock, Melissa L.; Shi, Jianhua; Tcherkezian, Joseph; Young-Pearse, Tracy L.; Flanagan, John G. APC Is an RNA-Binding Protein, and Its Interactome Provides a Link to Neural Development and Microtubule Assembly. Cell. 2014; 158:368–382. [PubMed: 25036633]

Noble M, Lewis SA, Cowan NJ. The microtubule binding domain of microtubule-associated protein MAP1B contains a repeated sequence motif unrelated to that of MAP2 and tau. J Cell Biol. 1989; 109:3367–76. [PubMed: 2480963]

Noiges R, Eichinger R, Kutschera W, Fischer I, Nemeth Z, Wiche G, Propst F. Microtubule-associated protein 1A (MAP1A) and MAP1B: light chains determine distinct functional properties. J Neurosci. 2002; 22:2106–14. [PubMed: 11896150]

Onifer SM, Smith GM, Fouad K. Plasticity after spinal cord injury: relevance to recovery and approaches to facilitate it. Neurotherapeutics. 2011; 8:283–93. [PubMed: 21384221]

Ponomareva OY, Holmen IC, Sperry AJ, Eliceiri KW, Halloran MC. Calsyntenin-1 regulates axon branching and endosomal trafficking during sensory neuron development in vivo. J Neurosci. 2014; 34(28):9235–48. [PubMed: 25009257]

Qiang L, Yu W, Liu M, Solowska JM, Baas PW. Basic fibroblast growth factor elicits formation of interstitial axonal branches via enhanced severing of microtubules. Mol Biol Cell. 2010; 21:334–44. [PubMed: 19940015]

Rochlin MW, Itoh K, Adelstein RS, Bridgman PC. Localization of myosin II A and B isoforms in cultured neurons. J Cell Sci. 1995; 108:3661–70. [PubMed: 8719872]

Roth AD, Liazoghli D, Perez De Arce F, Colman DR. Septin 7: actin cross-organization is required for axonal association of Schwann cells. Biol Res. 2013; 46:243–9. [PubMed: 24346071]

Sainath R, Gallo G. The Dynein Inhibitor Ciliobrevin D Inhibits the Bi-directional Transport of Organelles along Sensory Axons and Impairs NGF-Mediated Regulation of Growth Cones and Axon Branches. Dev Neurobio. 2014 In Press.

Spiliotis ET, Nelson WJ. Here come the septins: novel polymers that coordinate intracellular functions and organization. J Cell Sci. Jan 1; 2006 119(Pt 1):4–10. 2006. [PubMed: 16371649]

Spillane M, Ketschek A, Jones SL, Korobova F, Marsick B, Lanier L, Svitkina T, Gallo G. The actin nucleating Arp2/3 complex contributes to the formation of axonal filopodia and branches through the regulation of actin patch precursors to filopodia. Dev Neurobiol. 2011; 71:747–58. [PubMed: 21557512]

Spillane M, Ketschek A, Donnelly CJ, Pacheco A, Twiss JL, Gallo G. Nerve growth factor-induced formation of axonal filopodia and collateral branches involves the intra-axonal synthesis of regulators of the actin-nucleating Arp2/3 complex. J Neurosci. 2012; 32:17671–89. [PubMed: 23223289]

Spillane M, Ketschek A, Merianda TT, Twiss JL, Gallo G. Mitochondria coordinate sites of axon branching through localized intra-axonal protein synthesis. Cell Rep. 2013; 5:1564–75. [PubMed: 24332852]

Spillane M, Gallo G. Involvement of Rho-family GTPases in axon branching. Small GTPases. 2014 In Press.

Svitkina T. Imaging cytoskeleton components by electron microscopy. Methods Mol Biol. 2009; 586:187–206. [PubMed: 19768431]

Takei Y, Teng J, Harada A, Hirokawa N. Defects in axonal elongation and neuronal migration in mice with disrupted tau and map1b genes. J Cell Biol. 2000; 150:989–1000. [PubMed: 10973990]

Takemura R, Okabe S, Umeyama T, Kanai Y, Cowan NJ, Hirokawa N. Increased microtubule stability and alpha tubulin acetylation in cells transfected with microtubule-associated proteins MAP1B, MAP2 or tau. J Cell Sci. 1992; 103:953–64. [PubMed: 1487506]

Tao K, Matsuki N, Koyama R. AMP-activated protein kinase mediates activity-dependent axon branching by recruiting mitochondria to axon. Dev Neurobiol. 2014; 74:557–73. [PubMed: 24218086]

Teng J, Takei Y, Harada A, Nakata T, Chen J, Hirokawa N. Synergistic effects of MAP2 and MAP1B knockout in neuronal migration, dendritic outgrowth, and microtubule organization. J Cell Biol. 2001; 155:65–76. [PubMed: 11581286]

Tint I, Fischer I, Black M. Acute inactivation of MAP1b in growing sympathetic neurons destabilizes axonal microtubules. Cell Motil Cytoskeleton. 2005; 60:48–65. [PubMed: 15573412]

Trivedi N, Marsh P, Goold RG, Wood-Kaczmar A, Gordon-Weeks PR. Glycogen synthase kinase-3beta phosphorylation of MAP1B at Ser1260 and Thr1265 is spatially restricted to growing axons. J Cell Sci. 2005; 118:993–1005. [PubMed: 15731007]

Tymanskyj SR, Scales TM, Gordon-Weeks PR. MAP1B enhances microtubule assembly rates and axon extension rates in developing neurons. Mol Cell Neurosci. 2012; 49(2):110–9. [PubMed: 22033417]

Utreras E, Jiménez-Mateos EM, Contreras-Vallejos E, Tortosa E, Pérez M, Rojas S, Saragoni L, Maccioni RB, Avila J, González-Billault C. Microtubule-associated protein 1B interaction with tubulin tyrosine ligase contributes to the control of microtubule tyrosination. Dev Neurosci. 2008; 30(1-3):200–10. 2008. [PubMed: 18075266]

Villarroel-Campos D, González -Billault C. The MAP1B case: An old MAP that is new again. Dev Neurobiol. 2014; 74(10):953–71. [PubMed: 24700609]

Xu K, Zhong G, Zhuang X. Actin, spectrin, and associated proteins form a periodic cytoskeletal structure in axons. Science. 2013; 339:452–6. [PubMed: 23239625]

Yu W, Ahmad FJ, Baas PW. Microtubule fragmentation and partitioning in the axon during collateral branch formation. J Neurosci. 1994; 14:5872–84. [PubMed: 7931550]

Yu W, Qiang L, Solowska JM, Karabay A, Korulu S, Baas PW. The microtubule-severing proteins spastin and katanin participate differently in the formation of axonal branches. Mol Biol Cell. 2008; 19:1485–98. [PubMed: 18234839]

Zhao Z, Wang Z, Gu Y, Feil R, Hofmann F, Ma L. Regulate axon branching by the cyclic GMP pathway via inhibition of glycogen synthase kinase 3 in dorsal root ganglion sensory neurons. J Neurosci. 2009; 29:1350–60. [PubMed: 19193882]

Zhou FQ, Zhou J, Dedhar S, Wu YH, Snider WD. NGF-induced axon growth is mediated by localized inactivation of GSK-3beta and functions of the microtubule plus end binding protein APC. Neuron. 2004; 42(6):897–912. [PubMed: 15207235]

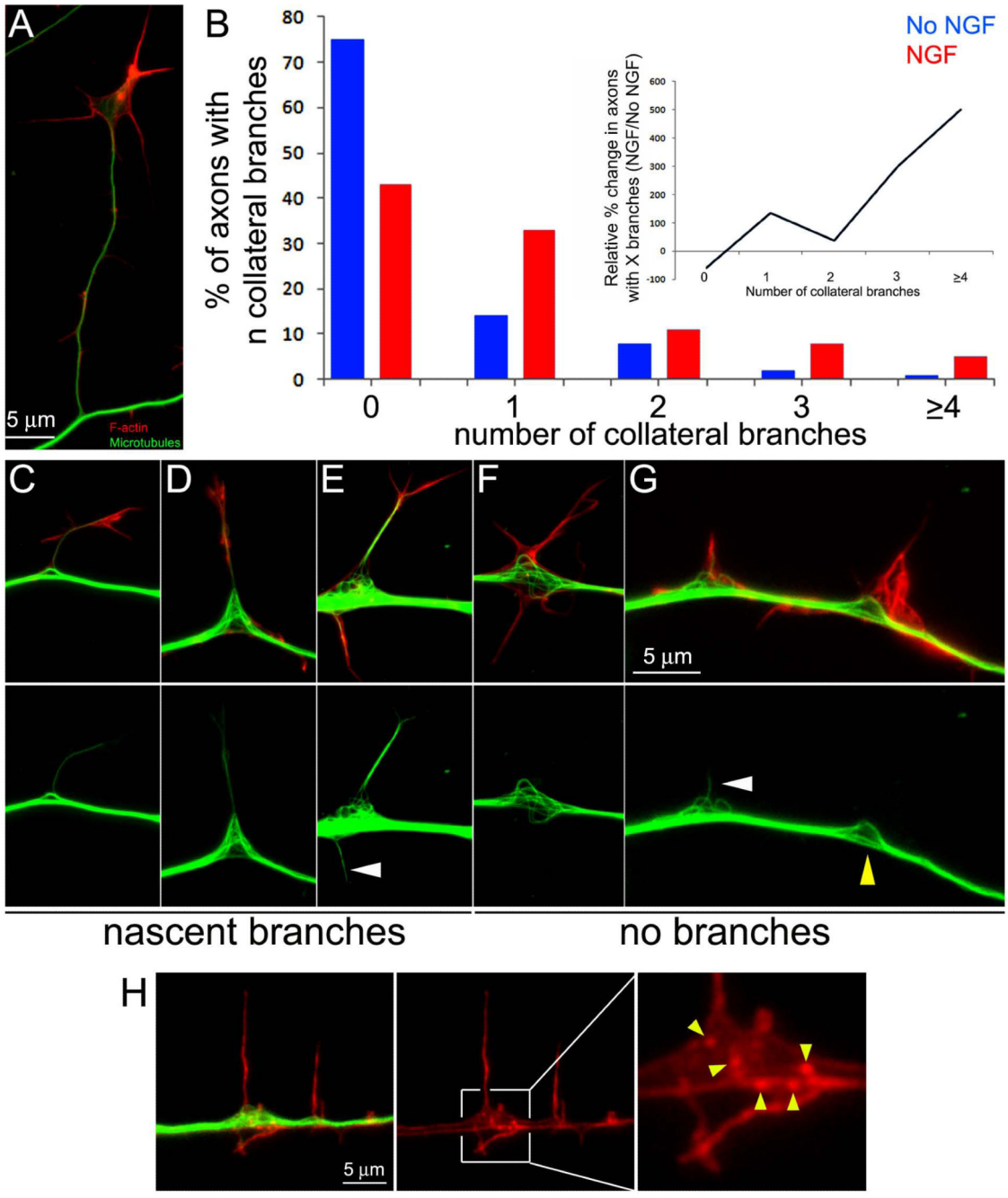

Figure 1.

NGF promotes axon collateral branching and localized reorganization of the axonal microtubule array. **(A)** Example of a mature collateral branch approximately 30 µm in length. Images show F-actin (red) and microtubules (green) in samples that were simultaneously fixed and extracted prior to staining, and the tubulin signal thus reflects microtubules. **(B)** Distributions of axons with the given number of collateral branches (x axis) in cultures treated with NGF for 30 min (red bars; n=121) or control treatment (blue bars; n=124). Inset shows the percent change induced by NGF within each bin of the number

of collaterals per axon relative to the control. NGF decreased the relative percentage of axons with 0 collaterals by 50%, but increased the relative percentage of axons generating 1 or more axons. **(C-E)** Examples of microtubule debundling at the base of nascent branches. **(F)** Example of bi-lateral microtubule debundling and splaying at a site exhibiting bi-lateral lateral filopodia. **(G)** Example of microtubule debundling and microtubule entry into an axonal filopodia (white arrowhead; also see panel E). The yellow arrowhead denotes a site of debundling correlating with axonal filopodia but not showing microtubule entry into the filopodia. **(H)** Example of actin patches at sites of microtubule debundling. The boxed in region encompassing the site of debundling is enlarged through empty magnification in the right-most panel and structures scored as actin patches are denoted by the yellow arrowheads.

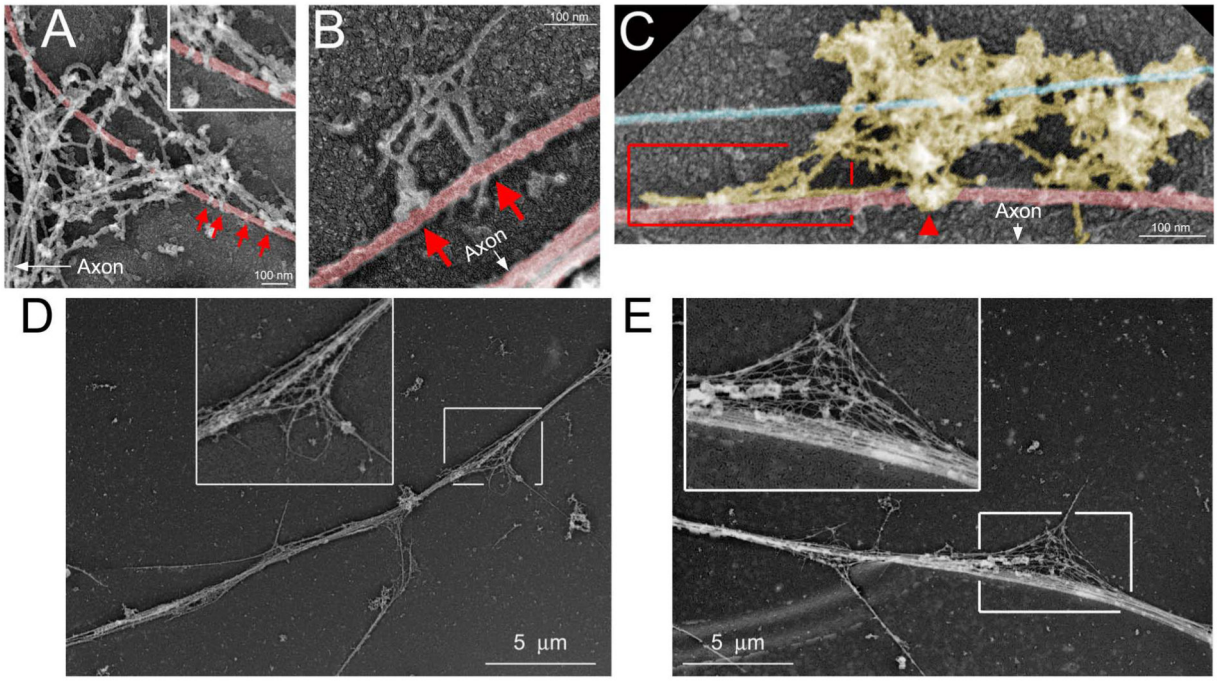

Figure 2.

Platinum replica electron microscopic analysis of the relationship between actin filaments and microtubules at sites of debundling. Microtubules shaded red, neurofilaments shaded blue, actin filaments not shaded. The arrows in (A-C) denote the location of the main axon relative to the close up views shown. **(A)** Example of a microtubule enmeshed in a patch of actin filaments at the base of a filopodium along the axon. The arrows point to apparent contacts between the ends of actin filaments and microtubules. The inset shows a further magnified view of the contacts. **(B)** Example of a few actin filaments associated with a debundled microtubule. Arrows point to apparent contacts between the ends of actin filaments and the microtubule. **(C)** Example of a patch of axonal actin filaments exhibiting a cluster around a microtubule (arrowhead) and becoming aligned with the axis of the microtubule (boxed in region). **(D)** and **(E)** show lower magnification examples of sites along the axon exhibiting the debundling of the microtubule array, as show at higher resolution in panels A-C. The insets denote the areas of debundling at 2× empty magnification.

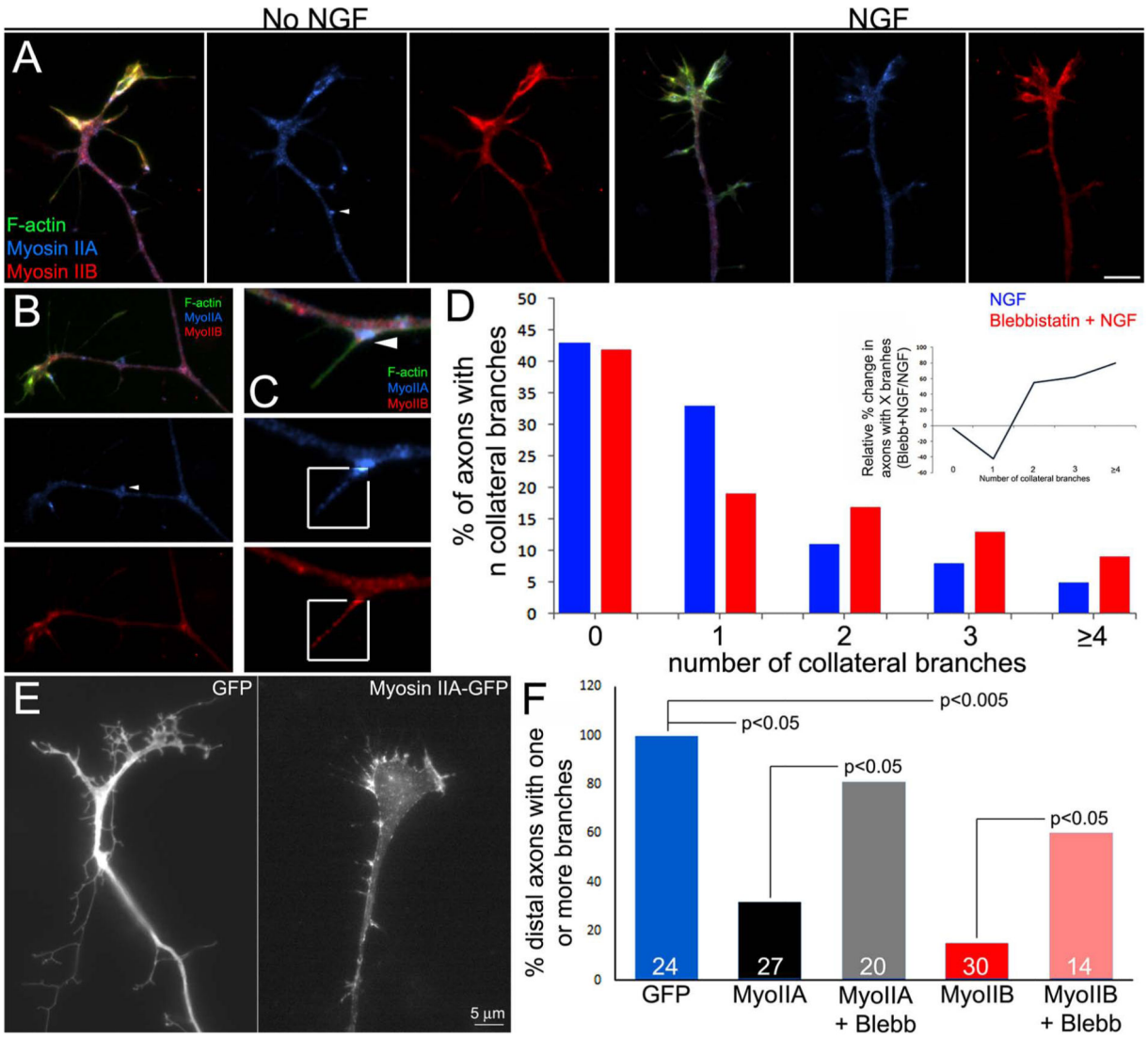

Figure 3.

Myosin II negatively regulates the collateral branching of sensory axons. **(A)** Distributions of myosin IIA and IIB in axons in the absence of NGF treatment and following NGF treatment. No clear differences in the levels or distribution of myosin II was observed. **(B)** Example of the distribution of myosin IIA and IIB in a mature collateral branch. As in the main axon, both myosins are found throughout the branch. **(C)** Myosin IIA showed accumulation at the base of subsets of filopodia, as shown in this example (arrowhead; also see arrowhead in panels A and B). Myosin IIA and IIB puncta were also found in filopodial shafts as shown in the boxed-in regions. The boxed in regions have been contrast enhanced to show the distribution of myosin IIA and IIB in filopodia, which is otherwise hard to detect while also keeping the rest of the axon, which has a much greater volume, below saturation. **(D)** Graph of the distribution of the number of collateral branches along distal axons after NGF treatment with and without treatment with 50 µM blebbistatin. The inset was prepared as described in Figure 1B. Relative to NGF treatment alone, blebbistatin cotreatment

increased the proportion of axons that generated multiple branches (≥2) and decreased the proportion that generated only one branch (inset graph), but did not affect the percentage of axons that formed ≥1 branches. **(E)** Examples of the distal axons of neurons transfected with GFP or myosin IIA-GFP. Over-expressed Myosin II exhibited a overall similar distribution as observed for the endogenous myosin. Expression of myosin IIB resulted in a similar distribution (not shown). **(F)** Quantification of the proportion of axons exhibiting one or more branches along the distal 50 μm. Overexpression of either myosin IIA or IIB decreased the proportion of axons exhibiting branches, and blebbistatin (50 μM) partially reversed the effects of myosin II overexpression. Data are normalized to the GFP group. n=axons shown in bars.

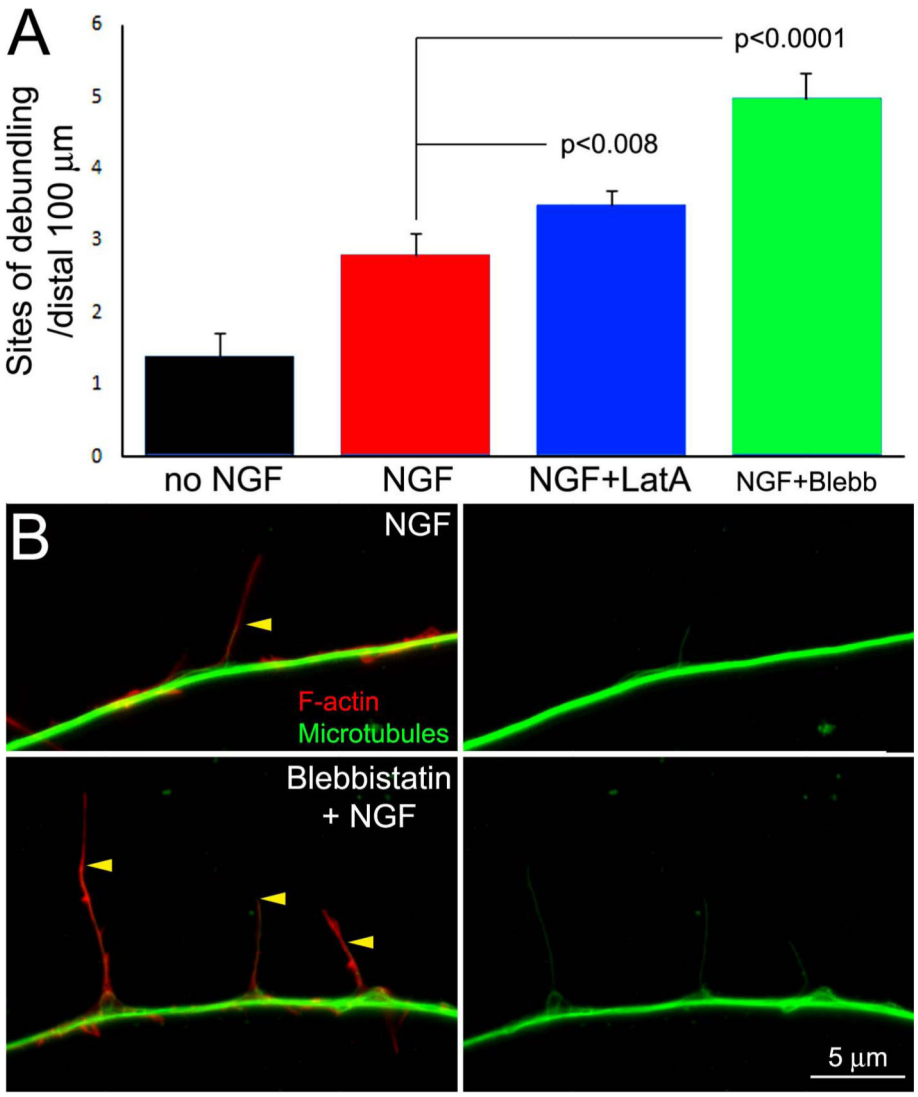

Figure 4.

Inhibition of myosin II activity and depolymerization of actin filaments promote NGF-induced microtubule debundling. **(A)** Graph showing the number of debundling sites per unit length of axons treated with NGF, and cotreated with the myosin II inhibitor blebbistatin (Blebb, 50 µM) or the actin filament depolymerizing agent latrunculin-A (LatA, 5 µM). **(B)** Examples of axons treated with latrunculin-A or blebbistatin. The } denote sites of microtubule debundling. Occasionally, segments of the axon containing accumulations of actin filaments (red arrowhead) were observed along latrunculin-A treated axons but did not correlate with sites of debundling. **(C)** Examples of the distribution of actin filaments (red) and microtubules (green) in axons treated with NGF or cotreated with NGF and blebbistatin. Yellow arrowheads show the positons of the distal tips of microtubules in filopodia.

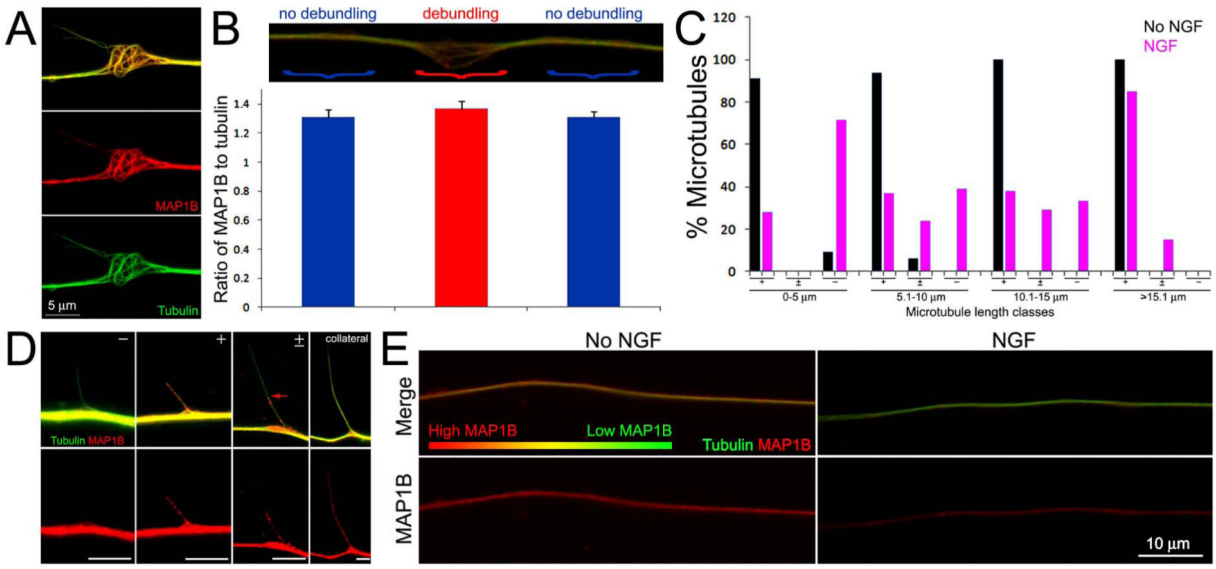

Figure 5.

Treatment with NGF alters the levels of microtubule associated MAP1B during early stages of collateral formation. **(A)** Example of MAP1B distribution at a site of microtubule debundling along an NGF treated axon. Note that MAP1B is found along the length of debundled and splayed microtubules. Image is contrast enhanced to highlight the relationship between individual microtubules and MAP1B. **(B)** Quantification of the ratio of MAP1B to tubulin staining in simultaneously fixed and extracted axons. The image shows the relative sites of measurement, denoted by }, and the according ratiometric measurements are shown in the graph below. Ratios were determined at the site of debundling (red) and adjacent distal and proximal segments of similar lengths (blue). The ratios were not statistically different (n=20 debundling sites from 20 axons; p=0.22 Kurskal-Wallis non-paramteric ANOVA). **(C)** Distributions of microtubules with tips extending outward from the axon shaft that exhibited MAP1B staining in no NGF (n=55) and NGF treatment (n=113) groups. +, ± and − denote categories of microtubules stained by MAP1B along their entire length, showing partial coverage and no MAP1B staining, respectively. See (D) for examples of these categories. The percent of microtubules falling into categories is shown as a function of the length of microtubules. **(D)** Examples of MAP1B staining patterns along microtubules. The categories (+,±,−) are denoted as in panel (C). The red arrow in the ± panel shows the extent of MAP1B staining. Bars = 5 µm. Images are contrast enhanced to best reveal relevant features (i.e., individual microtubules which would be of low intensity relative to the full array in the axon shaft). **(E)** Examples of the relative staining intensities of MAP1B and tubulin in simultaneously fixed and extracted axons. Raw data images are shown, all samples were stained in parallel and images acquired using identical acquisition protocols. The axon not treated with NGF exhibits more yellow color than the NGF treated axon, reflecting a greater level of MAP1B relative to tubulin than the NGF treated axon which appear greener. Individual MAP1B channels are shown in the bottom panels. The false color gradient bar provides a visual representation of the relative levels of MAP1B (red) to tubulin (green).

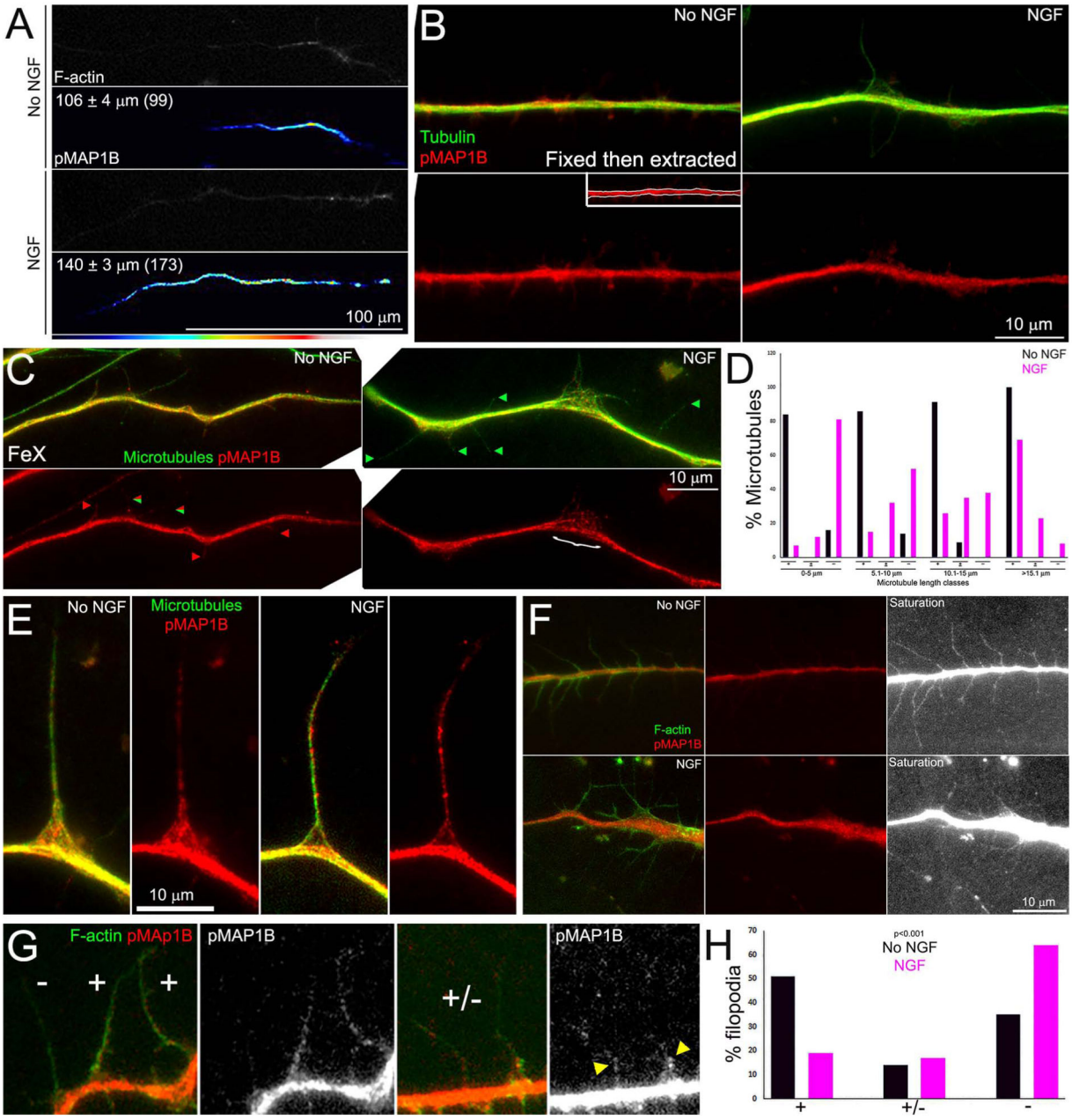

Figure 6.

Effects of NGF on the levels and distribution of pT1265-MAP1B along axons. **(A)** Examples of gradients of pT1265-MAP1B (pMAP1B) intensity along distal axons. The mean lengths of gradients are shown in the panels. For presentation, the pT1265-MAP1B images were subjected to decreased brightness modifications until the proximal segment of the axon that exhibited low constant levels of pT1265-MAP1B was no longer visible revealing only the distal gradient. **(B)** Examples of axons stained to reveal pT1265-MAP1B and total tubulin in fixed then extracted samples. The inset in the No NGF pMAP1B panel shows the region of interest defined as the axon shaft for quantitative measurements. **(C)** Examples of axons stained to reveal pT1265-MAP1B and microtubules (anti-α-tubulin) in FeX samples. Green

arrowheads denote examples of microtubules devoid of pT1265-MAP1B signal, red arrowheads denote microtubules exhibiting pT1265-MAP1B staining, and the mix red/green arrowhead shows an example of microtubule with partial coverage by pT1265-MAP1B. These represent the −,+ and ± categories in panel (D), respectively. The } in the NGF treated panel denotes a region of microtubule debundling. Note that debundled microtubules are decorated by pT1265-MAP1B. **(D)** Percentages of microtubules in given length classes that exhibited pT1265-MAP1B staining as a function of NGF treatment. The graph follows the format of Figure 5C. **(E)** Examples of collaterals in FeX samples. **(F)** Examples of axons fixed and then extracted and stained to reveal actin filaments, for direct visualization of filopodia, and pT1265-MAP1B. NGF treatment decreased the extent of pT1265-MAP1B staining in axonal filopodia. The “saturated” panels show the pT1265-MAP1B signal with the levels in the axon saturated (pure white) through increasing the brightness of the images to allow closer examination of the pT1265-MAP1B levels in the filopodia which are much dimmer than in the axon, likely due to volumetric differences. Both NGF and No NGF panels were identically manipulated to generate the saturated panels. Also note that in panel B protrusions are visible off the axon shaft of the No NGF example but only minimally the NGF treated example. **(G)** Examples of the categories used to score the presence of pT1265-MAP1B staining in axonal filopodia. The (+) category represents filopodia which exhibited pT1265-MAP1B staining over greater than 50% of the shaft. The (−) category reflects filopodia with minimal to undetectable pT1265-MAP1B staining. The yellow arrowheads in the right-most panel denote partial pT1265-MAP1B coverage at the base of filopodia (+/− category). **(H)** Percentage of filopodia exhibiting pT1265-MAP1B staining as defined in (G). n=208 and 212 filopodia in No NGF and NGF groups. Chi-squared test for independence.

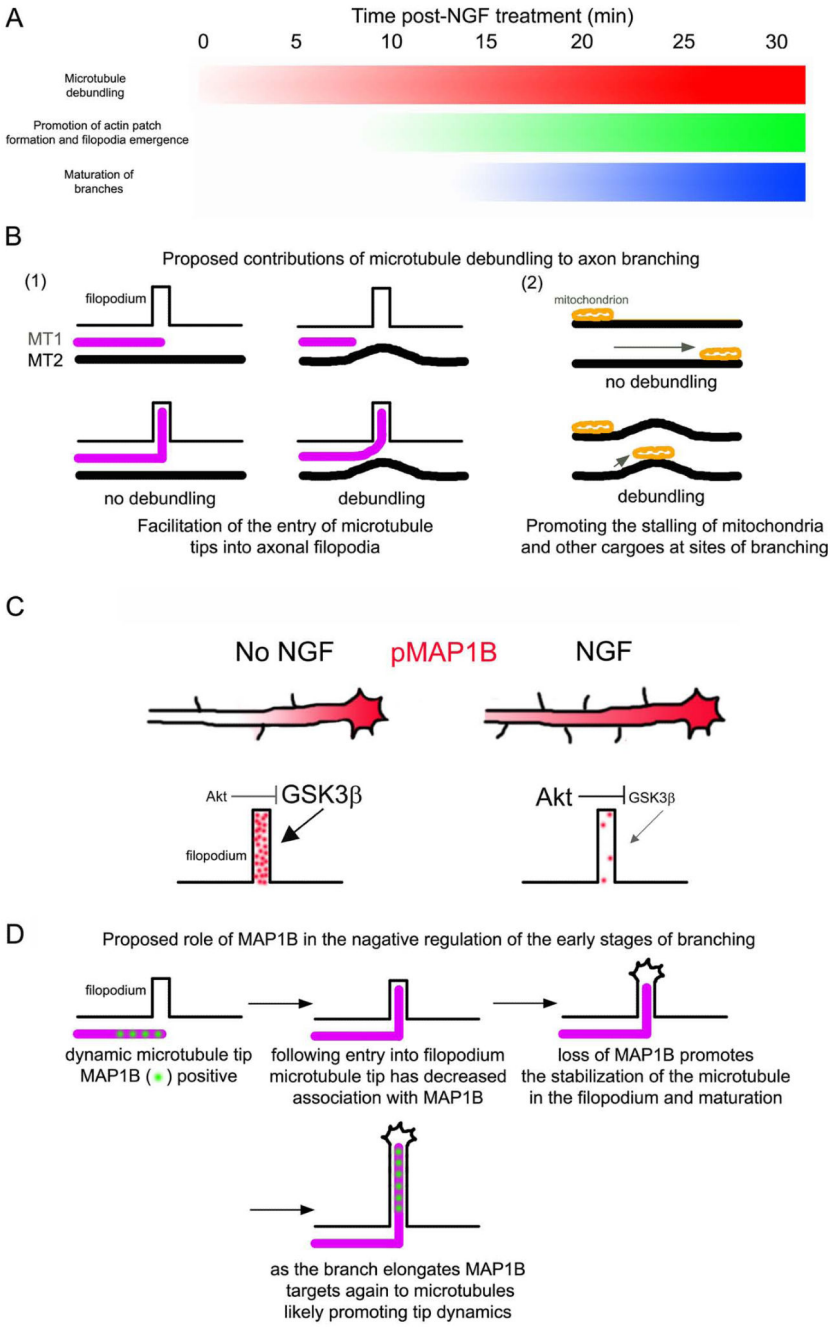

Figure 7.

Suggested working model for the role of sites of axonal microtubule debundling and MAP1B in the formation of collateral branches. **(A)** Diagram of the temporal sequence of cytoskeletal events during branching. The shaded regions reflect the relative prevalence of the event denoted on the left during the first 30 min of treatment with NGF, with white and black denoting minimal and maximal levels. The debundling of microtubules in response to NGF precedes the increases in the formation of axonal actin patches and filopodia (Spillane et al., 2012), consistent with sites of debundling being preferred sites for the formation of

filopodia and patches. Maturation of branches into filopodia begins to occur around 15 min post treatment with NGF and is maximal at 30 min (Spillane et al., 2012). Between 0-30 min NGF also drives the intra-axonal proteins synthesis of actin regulatory proteins in a manner dependent on mitochondria positioning and respiration (Spillane et al., 2012, 2013). **(B)** Proposed functions of the debundling of axonal microtubules during branching. (1) Two microtubules (MT) are shown in the proximity of a filopodium. MT1 has an actively polymerizing tip approaching the base of the filopodium. As noted in the discussion, microtubule tips polymerizing along the straight axis of the axon would have to make a near orthogonal turn into axonal filopodia. In the presence of debundled microtubules (e.g., MT2), microtubule tips may be aided in targeting to filopodia by being in part guided by the curved and debundled microtubules, thereby decreasing the angle the microtubule tip needs to achieve in order to enter the filopodium. (2) Curved microtubules may provide a less favorable substratum for motor-driven transport, resulting in more frequent stalling of cargoes at sites of microtubule debundling. Mitochondria stalling is a major component of the maturation of filopodia into branches (Courchet et al., 2013; Spillane et al., 2013; Tao et al., 2014). Thus, mitochondria may accumulate at sites of debundled microtubules, and indeed both sites of debundled microtubules and sites populated by stalled mitochondria are associated with the formation of axonal filopodia and branches (Spillane et al., 2013; Tao et al., 2014; current investigation). **(C)** Summary of the effects of NGF on pMAP1B levels along the axon shaft and within axonal filopodia. NGF increases the length of the pMAP1B gradient resulting in increased net levels of pMAP1B. However, in axonal filopodia, the levels of pMAP1B are locally decreased. Based on previous literature (see discussion) and the current study, we propose that local NGF signaling in filopodia decreases GSK3β activity through activation of PI3K-Akt signaling. The size of the text in the panel reflects relative activity levels of the kinases (Akt and GSK3β). **(D)** Proposed role of the decrease in MAP1B association with microtubules in axonal filopodia during the early stages of branching. Briefly, as MAP1B promotes microtubule tip polymerization, the data suggest that the decreased association of MAP1B with microtubules in axonal filopodia may, at least in part, increase their stability contributing the maturation of the filopodium into a branch. Once the branch has matured and established polarity (i.e., a small growth cone forms at its tip and the actin filament organization is no longer filopodial), MAP1B is again recruited to the microtubules within the branch where it may serve to promote microtubule polymerization during subsequent extension of the branch.